

Supplement of Atmos. Meas. Tech., 8, 2069–2091, 2015
<http://www.atmos-meas-tech.net/8/2069/2015/>
doi:10.5194/amt-8-2069-2015-supplement
© Author(s) 2015. CC Attribution 3.0 License.



Supplement of

Big grains go far: understanding the discrepancy between tephrochronology and satellite infrared measurements of volcanic ash

J. A. Stevenson et al.

Correspondence to: J. A. Stevenson (johnalexanderstevenson@yahoo.co.uk)

The copyright of individual parts of the supplement might differ from the CC-BY 3.0 licence.

Additional distal tephra grainsize distributions

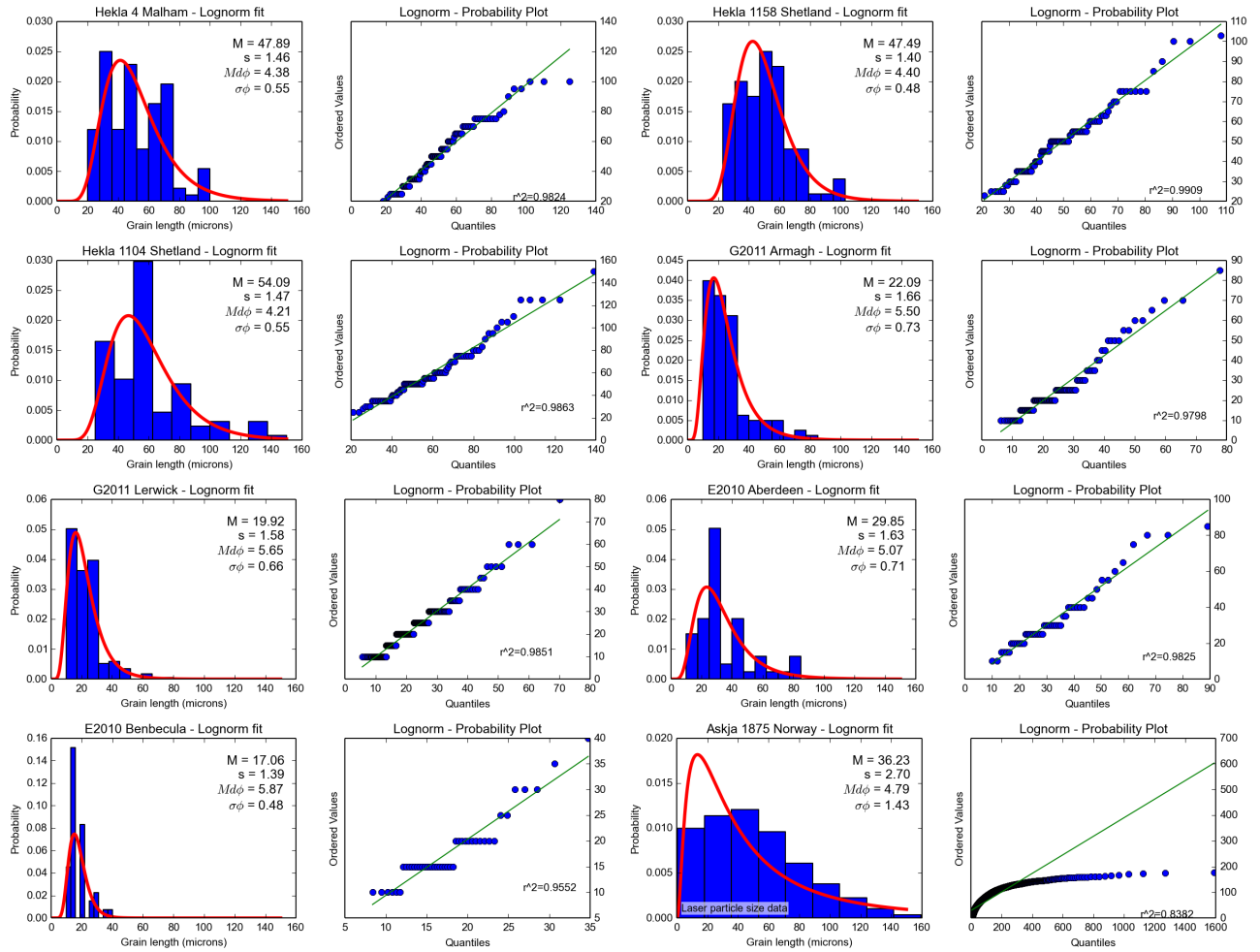


Figure 1: Further examples of statistical model fits to distal tephra grainsize distributions. Note the poor fit of the lognormal distribution to the laser particle size data.

Cryptotephra range for different compositions

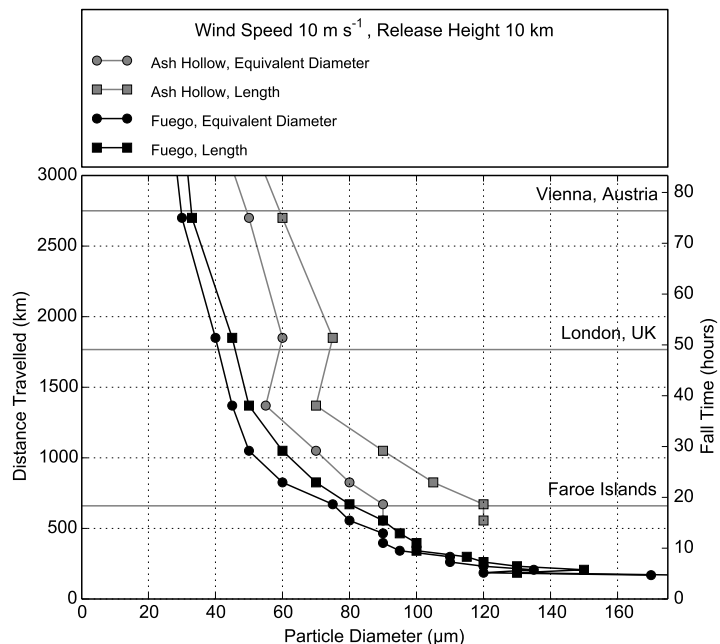


Figure 2: The effect of composition on cryptotephra range. Travel distance and travel time of Fuego (basaltic) and Ash Hollow (rhyolitic) ash particles using their measured fall velocities at sea level, where particle diameter is taken to be equivalent area diameter and long axis length. The grey horizontal lines represent the distances from Eyjafjallajökull to various European locations. Rhyolite grains travel further than basaltic grains.

Effect of *a priori* values on retrievals

In order to determine the effect of the *a priori* values on the retrievals, we calculated the averaging kernel and degrees of freedom of signal, based on the retrieval parameters described in Francis et al. (2012) and used by the London Volcanic Ash Advisory Centre (VAAC). The averaging kernel matrix is defined by Rodgers (2000) as:

$$\mathbf{A} = (\mathbf{K}^T \mathbf{S}_E^{-1} \mathbf{K} + \mathbf{S}_a^{-1})^{-1} \mathbf{K}^T \mathbf{S}_E^{-1} \mathbf{K} \quad (1)$$

where \mathbf{K} is the weighting function matrix, \mathbf{S}_E is the covariance of the measurement noise and \mathbf{S}_a is the covariance of the prior estimate of the state. The diagonal elements of the averaging kernel indicate, for each variable, the fraction of the retrieved state that is determined by the true value as given by the observations. The rest is determined by the *a priori* value and the other elements of the state vector (Thomas et al., 2009). For a perfect retrieval system \mathbf{A} is an identity matrix. The trace of \mathbf{A} gives the degrees of freedom of signal; this describes the number of useful independent quantities that can be extracted from the measurements (Rodgers, 2000).

Here, the state vector contains three quantities: the ash layer pressure (p_{ash} ; a proxy for the altitude of the cloud), the ash column mass loading (L), and the ash size distribution effective radius (r_{eff}). \mathbf{A} is a 3×3 matrix whose diagonal elements are the averaging kernel elements for ash layer pressure, mass loading and effective radius. The sum of these values is the degrees of freedom of signal. Fig. 3 shows how the degrees of freedom of signal and the effective radius element of the averaging kernel vary over the range of input mass median radii (i.e. PSD) and ash column mass loading used in the simulated images.

Overall, the observations have a strong impact on the retrievals with median averaging kernel elements of 0.95 for effective radius and 0.97 and 0.84 for mass loading and ash layer pressure (not shown), respectively. The corresponding median degrees of freedom of signal is 2.7 (out of a possible 3), indicating that between two and three independent pieces of information can be retrieved. The problem is therefore under-constrained and the retrieved values are partly dependant on their *a priori* estimates. This effect varies depending on the true state values. In general, small particle sizes and large mass loadings have a greater value of the effective radius averaging kernel element, \mathbf{A}_{reff} . The observations have the greatest impact on the retrievals in these cases. As the particle size increases and/or the mass loading decreases, \mathbf{A}_{reff} decreases, and the *a priori* values become more important. This illustrates the reduced sensitivity of the retrievals to larger particles.

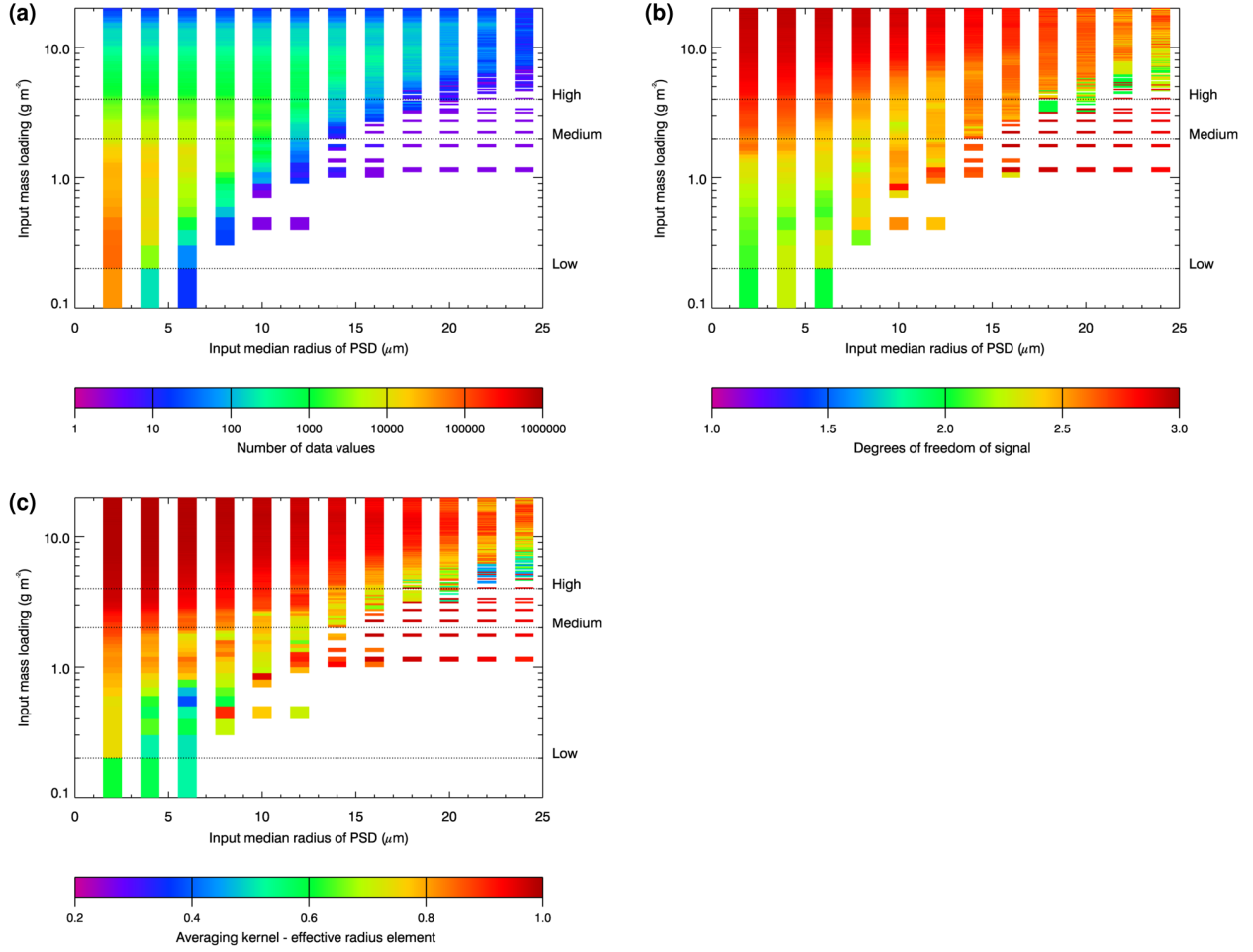


Figure 3: Effect of median radius and mass loading on retrieval sensitivity, based on retrievals from simulated satellite images using the London VAAC operational settings as described by Francis et al., (2012). The horizontal lines show the mass loadings that, assuming a 1 km thick ash cloud, correspond to the volcanic ash concentrations that define zones of low, medium and high contamination (0.2 , 2 and 4 mg m^{-3}). (a) Number of retrieved data points for each size and mass loading. The range of input mass loading values are controlled by the NAME model. The number of retrieved values depends on the number of ash-containing pixels that were identified. The number of retrieved pixels decreases as the input mass median radius increases, particularly above $6 \mu\text{m}$. (b) Median degrees of freedom of signal for retrieved pixels. The retrieved parameters are most sensitive to finer particles (mass median radius $< 6 \mu\text{m}$) and high mass loadings ($> 2 \text{ g m}^{-2}$). Even for the finest particles, the *a priori* values become more important as the mass loading decreases. (c) Median effective radius averaging kernel element for retrieved pixels. As with the degrees of freedom of signal, the retrieval is most sensitive to small particles at large mass loadings. At lower concentrations, the retrieved effective radius becomes more sensitive to the *a priori* values and the other parameters. In these situations, using a low *a priori* effective radius will lead to under estimation of the particle size.